Inorganic Chemistry

pubs.acs.org/IC

Article

Tethered Alkylidenes for REMP from Carbon Disulfide Cleavage

Vineet K. Jakhar, Yu-Hsuan Shen, Rinku Yadav, Soufiane S. Nadif, Ion Ghiviriga, Khalil A. Abboud, Daniel W. Lester, and Adam S. Veige*

Cite This: *Inorg. Chem.* 2024, 63, 12207−12217

ABSTRACT: Reactions between tungsten alkylidyne [^{t}BuOCO]-W≡C^{t}Bu(THF)$_2$ **1** and sulfur containing small molecules are reported. Complex **1** reacts with CS_2 to produce intermediate η^2 bound CS_2 complex [O_2C(^{t}BuC=)W(η^2-(*S*,*C*)-CS_2)(THF)] **8**. Heating complex **8** provides a mixture of a monomeric tungsten sulfido complex **9** and a dimeric complex **10** in a 4:1 ratio, respectively. Heating the mixture does not perturb the ratio. Addition of excess THF in a solution of **9** and **10** (4:1) converts **10** to **9** (>96%) with concomitant loss of $(CS)_x$. Both **9** and **10** can be selectively crystallized from the mixture. An alternative synthesis of exclusively monomeric **9** involves the reaction between **1** and PhNCS. Demonstrating ring expansion metathesis polymerization (REMP), tethered tungsten alkylidene **8** polymerizes norbornene to produce *cis*-selective *syndiotactic* cyclic polynorbornene (*c*-poly(NBE)).

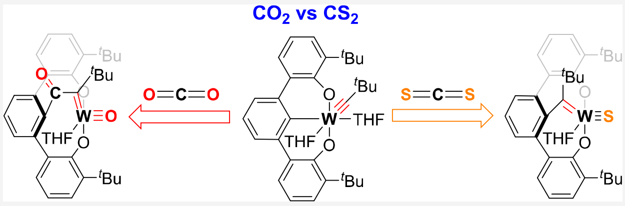

■ INTRODUCTION

In 2016, we reported the CO_2 cleavage reaction promoted by the trianionic (OCO^{3-}) pincer-supported tungsten alkylidyne **1**[1,2] to generate the tungsten oxo alkylidene **2** and dimer **3** in a 9:2 ratio, respectively (Scheme 1).[3] The unprecedented carbon dioxide C−O bond cleavage by an alkylidyne generates complex **2** that contains a tethered M=C bond. Catalyst **2** produces >98% *cis*, > 98% syndiotactic *c*-poly(NBE) via ring expansion metathesis polymerization.[4]

Scheme 1. Previously Reported Synthesis of Complexes (2) and (3)

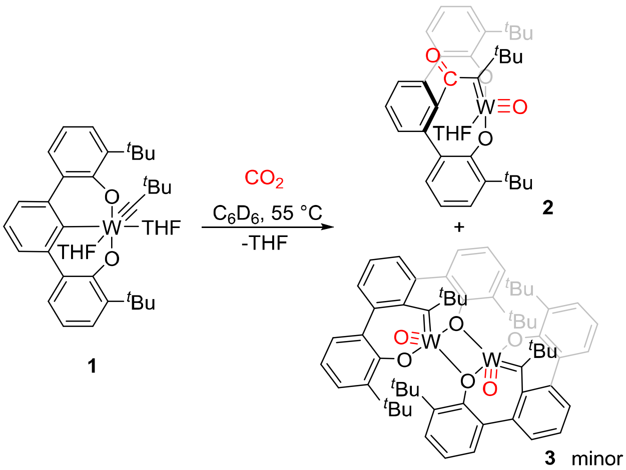

In 2021, we reported the reactivity of complex **1** with isocyanates (R−N=C=O), unsymmetrical analogues of carbon dioxide (Scheme 2).[5] Allowing for a broad range of variations not possible with carbon dioxide, isocyanates enable tuning of catalyst activity by changing the pendant imido-R-substituent. Despite both C=N and C=O double bonds

Scheme 2. Previously Reported Synthesis of Complexes 4-R and 5-NR (R = ^{t}Bu, Cy, and Ph)

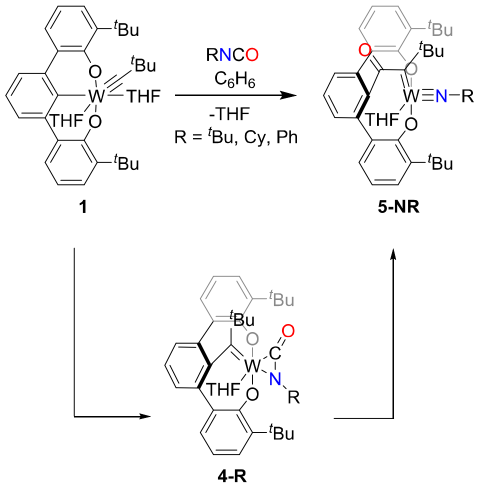

Received: April 13, 2024
Revised: May 28, 2024
Accepted: June 7, 2024
Published: June 18, 2024

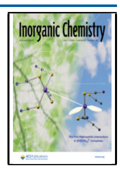

https://doi.org/10.1021/acs.inorgchem.4c01522
Inorg. Chem. 2024, 63, 12207−12217

being present in isocyanates, complex **1** reacts with RNCO (R = ^{t}Bu, Cy, and Ph) to exclusively cleave the C═N bond, yielding tethered tungsten-imido alkylidenes **5-NR**. Tethered tungsten-imido alkylidene **5-NR** contains an active tethered M═C bond and polymerizes norbornene to yield a highly stereoregular *c*-poly(NBE). Along the pathway to form **5-NR**, the η^2-(*N*,*C*)-isocyanate complex **4-R** was isolated. Complex **4-R** is noteworthy as an intermediate on the path to **5-NR** but also is an active initiator that polymerizes norbornene via ring expansion metathesis polymerization (REMP) to give high stereoregular *c*-poly(NBE) (>99% *cis* and syndiotactic).[6−9]

Tungsten alkylidyne complex **1** also reacts rapidly with organic azides to form tungsten azoimido complexes **6-N$_3$R** (Scheme 3).[10] Due to its inherent instability toward dinitrogen

Scheme 3. Previously Reported Synthesis of Complexes 6-N$_3$R and 7-NR (R = ^{t}Bu, Cy, Ph, Bz, TMS)

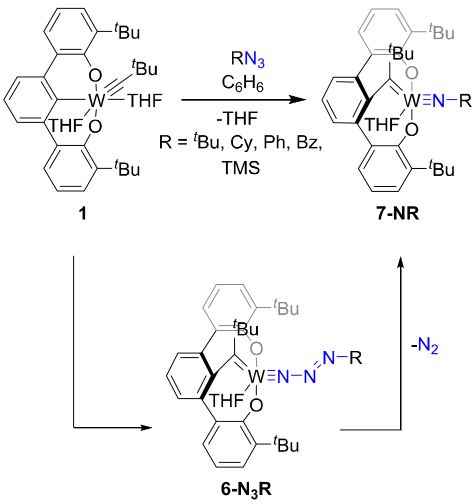

expulsion, the azoimido functional group is an uncommon ancillary ligand in polymer initiator design, yet complex **6-N$_3$R** is one of the best initiators for REMP. In fact, complexes **6-N$_3$R** are the only examples of initiators bearing an azoimido functional group. Again, seemingly a common occurrence, **6-N$_3$R** is an intermediate on a pathway to a more stable species. Loss of N_2 provides the corresponding imido complexes **7-NR** that are also REMP initiators.[10]

While the imido ligands in catalysts **5-NR** and **7-NR** allow for extensive variations, including the chain length and strain within the tethered alkylidene, the corresponding oxo ligand in catalyst **2** lacks variability. Presented herein, we replace the oxo with the isolobal, isoelectronic, and isosteric sulfido ligand by treating complex **1** with CS_2. The interesting feature of this work is that the reactivity profile of alkylidyne **1** completely changes by switching from CO_2 to CS_2.

Previous reports on the reaction between metal−carbon triple bonds and CS_2 are somewhat limited and reveal disparate results. In 1993, Mayr et al. reported the formation of alkynyl trithiocarbonato tungsten complexes [WX(PhCCSC(S)S)(CO)(PMe$_3$)$_2$] from [W(≡CPh)X(CO)(PMe$_3$)$_3$] (X = halide, SR) and CS_2 (Scheme 4A).[11] An alkylidyne thiocarbonyl tungsten complex was postulated as an intermediate in the reaction. In 1996, Hill et al. treated a solution of [Ru(≡CPh)Cl(CO)(PPh$_3$)$_2$] with CS_2 to afford the thiobenzoyl complex [Ru(η^2-SCPh)Cl(CS)(PPh$_3$)$_2$] (Scheme 4B).[12] The orientation of CS_2 addition is opposite to that observed in the analogous reaction with group 6 alkylidyne complexes. Subsequently, in 1997, Hill et al. reported the formation of an unusual metallacyclic thioketene complex that results from the reaction of [Mo(≡CR)(CO)(L)(Tp)] (R = C_6H_4-*p*-Me; L = CO, PPh$_3$; Tp = HB(pz)$_3$) with CS_2 (Scheme 4C).[13] The authors suggest that the first step involves a [2 + 2]-cycloaddition of Mo≡C and C═S, the regiochemical reverse of what is observed for the ruthenium alkylidyne complex, further supporting alternative modes of reactivity for early and late transition metal alkylidynes with CS_2. These examples illustrate the wide variety of C−S bond-forming reactions observed upon the treatment of alkylidynes with CS_2.

Exemplifying the diversity of the reactivity of CS_2 with alkylidynes, this study reveals unprecedented reaction pathways between alkylidyne **1** and CS_2. Included in this work is the synthesis of the first tethered tungsten sulfido alkylidene

Scheme 4. Reactions of Alkylidyne Complexes with CS_2

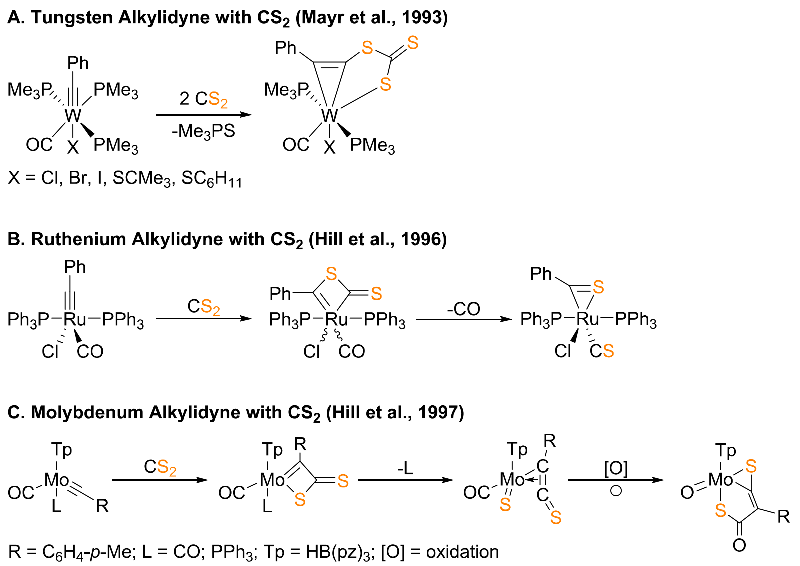

https://doi.org/10.1021/acs.inorgchem.4c01522
Inorg. Chem. 2024, 63, 12207−12217

and η^2-(*S*,*C*)-CS_2 complexes. Moreover, adding to the growing list of catalysts capable of REMP, the η^2-(*S*,*C*)-CS_2 complex is an active initiator for the synthesis of stereoregular *c*-poly(NBE).

■ RESULTS AND DISCUSSION

Treating a dark red toluene-d_8 solution of tungsten alkylidyne **1**[1] with 1.05 equiv of CS_2 results in an immediate color change to dark brown. The color change signifies the formation of the tetraanionic pincer complex [O_2C(^{t}BuC═)W(η^2-(*S*,*C*)-CS_2)(THF)] (**8**) (Scheme 5).

Scheme 5. Synthesis of Complex 8 by Reacting Complex 1 with CS_2

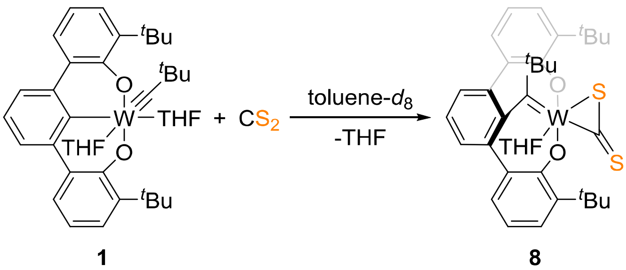

A combination of ^{1}H, ^{13}C{^{1}H}, gHSQC, and gHMBC NMR spectroscopy, single crystal X-ray diffraction (XRD), IR, and electrospray ionization mass spectrometry (ESI-MS) permits the unambiguous identification of complex **8**. However, attempts to isolate complex **8** were unsuccessful; multiple products form, presumably from the loss of THF from the tungsten center during evaporation of the solvent under vacuum. Despite its sensitivity to vacuum, single crystals amenable to XRD interrogation deposit from a concentrated hexane solution of **8** at −35 °C. Figure 1 depicts the solid-state molecular structure of **8**.

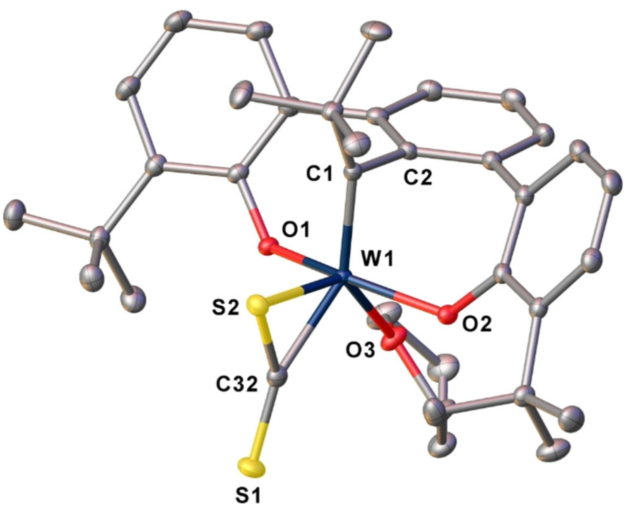

Figure 1. Solid-state structure of **8**. The hydrogen atoms are removed for the sake of clarity. Selected bond distances [Å]: W1−C1 1.9103(13), W1−S2 2.3396(3), W1−C32 2.0877(14), W1−O1 1.9654(9), W1−O2 1.9686(9), and W1−O3 2.2373(10). Selected bond angles [°]: ∠O1−W1−O2 152.90(4), ∠C1−W1−O3 134.55(5), ∠C1−W1−S2 86.89(4), ∠C1−W1−C32 131.55(5), ∠S1−C32−S2 138.94(9), and ∠S1−C32−W1 145.48(8).

Occupying three vertices, the pincer ligand binds in a tridentate *tetraanionic* form through two phenolate donors and an alkylidene. The η^2-(*S*,*C*)-CS_2 ligand and THF occupy the remaining vertices. The solid-state structure confirms that the alkylidyne present in complex **1** undergoes a formal reductive migratory insertion into the pincer-W-arene bond with a concomitant oxidative addition of C═S on the tungsten center. Similar alkylidyne insertions with complex **1** occur with organic azides,[10] phosphaalkyne,[14] isocyanates,[5] alkenes,[15,16] and alkynes.[17−19]

The W1═C1 bond length of 1.9103(13) Å within **8** is significantly longer than the W≡C bond length of 1.759(4) Å observed in complex **1**[1] and is comparable to other tetraanionic W(VI) tethered alkylidenes that range between 1.876(11) and 1.960(16) Å.[3,5,16−19] Evidenced by a long W1−O3 bond length of 2.2373(10) Å and presaging its sensitivity to vacuum, the coordinated THF experiences a strong *trans* influence. For comparison, the THF ligands in complex **1** are labile and have long W−O bonds (2.473(2) and 2.177(2) Å), with the longest being *trans* to the alkylidyne.[1] Signaling substantial back-donation of electron density from the tungsten center into the π^* orbital of the ligated C═S unit, the coordinated S2−C32 bond elongates to 1.6986(14) Å, and the S1−C32−S2 angle bends to 138.94(9)° (CS_2: C═S = 1.552(3) Å; S═C═S = 180°).[20] These structural features are consistent with related η^2-CS_2 complexes.[21−30] To the best of our knowledge, complex **8** is the first structurally characterized complex of a tungsten η^2-(*S*,*C*) coordinated CS_2. Though Schenk and co-workers reported the initial synthesis of a series of complexes with η^2-(*S*,*C*) coordination to a tungsten center [W(CO)$_3$(diphosphine)(CS_2)] and studied their reactivity toward various nucleophiles and electrophiles, no X-ray structural data exists.[31−33]

In agreement with the solid-state structure, the solution-phase ^{1}H NMR data exhibit resonances consistent with C_s-symmetry. Two singlets attributable to the ^{t}Bu protons of the pincer and alkylidene appear at 1.18 and 0.91 ppm, respectively. In the ^{13}C{^{1}H} NMR spectrum, the alkylidene carbon (W═*C*) resonates at 271.3 ppm, consistent with known pincer-supported tethered *tetraanionic* alkylidene complexes.[3,5,10,14,16−19,34] For reference, the alkylidyne carbon (W≡*C*) in complex **1** resonates at 320.7 ppm.[1] A resonance at 118.3 ppm for **8** corresponding to the C_{ipso} carbon indicates that the central aryl ring of the pincer is not directly attached to the W(VI) metal center, as the C_{ipso}-W resonance typically appears downfield near 200 ppm. Free $^{13}CS_2$ exhibits a ^{13}C{^{1}H} NMR resonance at 192.6 ppm for the C atom (S═^{13}C═S) in toluene-d_8. In complex **8**, the resonance corresponding to the carbon atom of the CS_2 group appears at 308.6 ppm. This downfield shift indicates a decrease in electron density upon coordination of CS_2 to a Lewis acidic metal center and supports the η^2-(*S*,*C*) coordination to the formal W(VI) ion. Further support for the assignment comes from a ^{13}C-enriched (97−99% ^{13}C) sample of **8′** featuring an intense resonance at 308.6 ($^2J_{W,C}$ = 90.6 Hz) ppm. Previously reported complexes containing η^2-(*N*,*C*) bound ^{t}BuNCO and η^2-(*P*,*C*) bound P≡C-Ad exhibit similar downfield resonances at 202.3 ppm (^{t}BuN═*C*═O)[5] and 299.8 ppm (d, $^1J_{C,P}$ = 103.2 Hz) (P≡*C*-Ad).[14]

In addition to the structural data for complex **8**, a solution-phase IR spectroscopy study is also consistent with a η^2-(*S*,*C*) bound CS_2 ligand. Two bands are associated with a η^2-(*S*,*C*) bound CS_2 ligand at 1158 and 680 cm^{-1} that shift to 1117 and

https://doi.org/10.1021/acs.inorgchem.4c01522
Inorg. Chem. 2024, 63, 12207−12217

658 cm^{-1} upon substitution by $^{13}CS_2$ in the IR spectrum of **8**. These signals are an out-of-ring $\nu_{C=S}$ stretching vibration and a ν_{C-S} bending vibration, respectively. The bands are considerably lower in energy than that of free $^{12}CS_2$ (ν_{as}: 1533 cm^{-1}), again reflecting the activation of CS_2.

Heating complex **8** in toluene-d_8 or simply combining complex **1** with CS_2 at 80 °C for 10 h, followed by addition of THF, provides the tungsten sulfido complex **9** in >96% yield. An alternative synthesis of **9** was found (Scheme 6). Treating **1** with PhNCS also generates **9** via S atom transfer. Adding PhNCS to a dark red solution of **1** causes an immediate color change from dark red to dark brown. Complex **9** forms within a few minutes. The yield of complex **9** in the reaction mixture, based on NMR, is ~65%. Thioisocyanates are sulfur atom transfer reagents that yield the corresponding isocyanides as byproducts.[35−37] However, a ^{1}H NMR spectrum of the reaction mixture did not reveal PhNC resonances; presumably the PhNC is consumed in side reactions with complex **1**. Confirming the side reactions, in a test reaction, treating **1** with PhNC in C_6D_6 results in a complicated mixture of products (NMR spectroscopy) (Figure S18). Unlike **8**, **9** is not sensitive to THF loss and is isolable as a solid. Complex **9** is also C_s-symmetric in solution. A ^{1}H NMR spectrum of **9** (benzene-d_6) displays two singlets for the aryl-^{t}Bu protons and the alkylidene ^{t}Bu protons in a 2:1 ratio at 1.75 and 0.96 ppm, respectively. In the ^{13}C NMR spectrum, a downfield resonance at 281.8 ppm is attributable to the alkylidene carbon (W═C) and is consistent with previously reported tethered tetraanionic alkylidene complexes.[3,5,16−19,34] Multinuclear ^{1}H−^{13}C HMBC displays a cross-peak between the C_{ipso} carbon and W═CC(CH_3) protons.

Scheme 6. Two Independent Syntheses of Tethered Sulfido 9

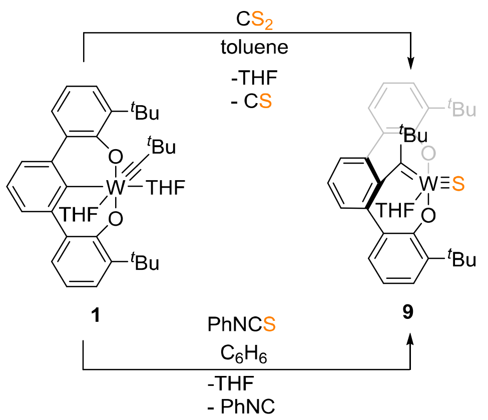

Single crystals deposit from a concentrated Et_2O solution of **9** at −35 °C. The tungsten ion in complex **9** (Figure 2) is square pyramidal (τ = 0.13).[38] The sulfido group occupies the axial position (W1−S1: 2.1257(8) Å), and the alkylidene (W1═C1: 1.876(3) Å), THF, and two aryloxides reside in the basal plane.

The W1═C1 bond length is 1.876(3) Å and lies within the range of previously reported *tetraanionic* pincer W(VI) alkylidene complexes.[3,16−18,34] Although not perfectly *trans* to the tungsten alkylidene, the THF again experiences a strong *trans* influence, manifesting in a long W1−O3 bond length of 2.212(2) Å. The alkylidene bond length in complex **9** is significantly shorter than those of the tethered tungsten oxo and imido alkylidene complexes, **2** and **5-N^{t}Bu**, (1.876(3) versus 1.9503(19)[3] and 1.9568(13)[5] Å). The W−O bond length of the THF *trans* to the alkylidene (2.212(2) Å) in complex **9** is also shorter than those in complex **2** (2.2689(15) Å)[3] and **5-N^{t}Bu** (2.3023(10) Å).[5] As expected, the W≡S bond (2.1257(8) Å) is considerably longer than the W≡O bond (1.6948(15) Å)[3] and W≡N bond (1.7302(11) Å).[5,10,39] The W≡S bond in complex **9** is comparable to previously reported neutral tungsten sulfido alkylidene NHC complexes (2.1150(8) and 2.1037(8) Å).[40] However, the alkylidene bond length in complex **9** is slightly shorter than the analogous neutral tungsten sulfido alkylidene NHC complexes (1.876(3) versus 1.936(3) and 1.882(3) Å).[40] In addition to the structural data for complex **9**, solution-phase IR spectroscopy further supports the presence of the terminal tungsten−sulfur (W1−S1) with a strong band at 525 cm^{-1}. Support for this assignment comes from known $\nu_{W≡S}$ stretching frequencies, typically in the range of 500−570 cm^{-1}.[41,42]

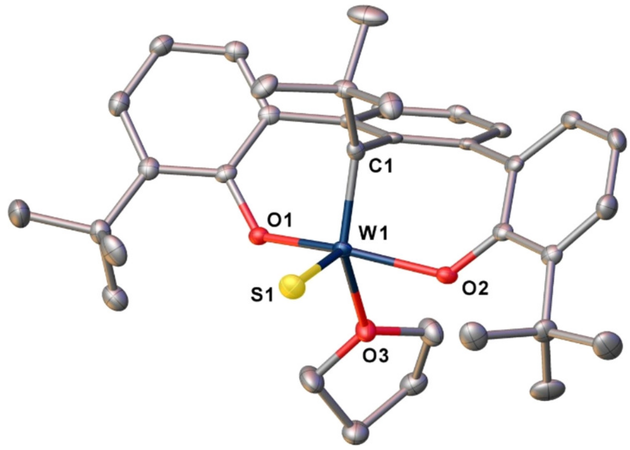

Figure 2. Solid-state structure of compound **9**. The hydrogen atoms are removed for clarity. Selected bond distances [Å]: W1−S1 2.1257(8), W1−C1 1.876(3), W1−O1 1.989(2), W1−O2 1.993(2), and W1−O3 2.212(2). Selected bond angles [°]: ∠C1−W1−O1 94.82(11), ∠O1−W1−O2 149.12(8), ∠C1−W1−S1 103.31(9), ∠O1−W1−S1 103.00(6), ∠C1−W1−O3 138.8(1), ∠O1−W1−O3 77.95(8), and ∠S1−W1−O3 117.87(6).

Using slightly different conditions, heating complex **8** in toluene-d_8 or simply combining complex **1** with CS_2 at 80 °C for 10 d but not adding THF generates dimer **10** as a minor component (1:4) of a mixture with sulfido **9** (Scheme 7). The solution color changes from dark brown to dark black-brown, and a small amount of precipitate forms, indicating the formation of $(CS)_x$ polymer.[43,44] Further heating the reaction mixture at 80 °C for 1 month does not change the ratio of complexes **9** and **10**, as monitored by NMR spectroscopy. However, adding an excess of THF to the reaction mixture converts complex **10** to complex **9** (>96%).

Complex **10** could not be isolated in pure form, but single crystals deposit from the reaction mixture. Specifically, evaporating all volatiles from the reaction mixture and triturating with pentane yields a brown-black solid. Dissolving the solid in excess pentane and filtering afforded a crude mixture of impure minor dimer product (complex **10**). Single crystals of **10** deposit from a concentrated solution of the mixture in toluene at ambient temperature. Figure 3 depicts the solid-state structure of complex **10**.

https://doi.org/10.1021/acs.inorgchem.4c01522
Inorg. Chem. 2024, 63, 12207−12217

Scheme 7. Formation of Intermediate 10 on the Pathway to Sulfido 9

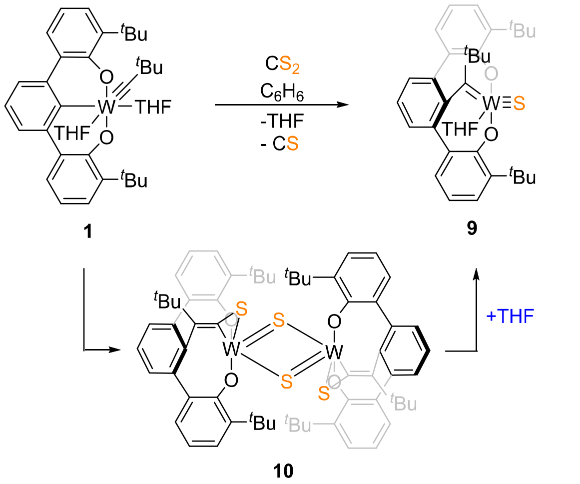

In contrast to the formation of the tungsten oxo dimer (complex **3**),[3] where CO is lost from the tethered backbone, CS remains in the tungsten sulfido dimer framework (Figure 3). The geometry around the tungsten center is distorted octahedral with two bridging sulfido ligands (considering the thiocarbonyl unit as a bidentate ligand). The W-μ-S bond distances (W1−S1 2.482(10) and W1−S1′ 2.356(8); W1′−S1 2.349(8) and W1′−S1′ 2.488(10) Å) reflect the asymmetrical nature of the bridging sulfur atoms bonded to the tungsten centers (Figure 3). For comparison, the typical W−S single bond length is 2.39 Å.[45,46] The W−W distance of 3.442 Å falls outside the range of 2.871−3.027 Å for the subset of $W_2(\mu\text{-}S)_2$ species in a + 6-oxidation state,[47] indicating weak or negligible direct metal−metal bonding. The W_2S_2 ring is puckered slightly with a dihedral angle of 11.4°, defined by W1−S1−W1′ and W1−S1′−W1′ planes. These structural features are comparable with other $W_2(\mu\text{-}S)_2$ cores.[47−61]

In contrast to the rich organometallic chemistry of ketenylide complexes,[3,5,62−74] the chemistry of thioketenyl complexes is limited to a few structurally characterized complexes.[75,76] The S2−C1 bond length 1.701(7) Å indicates multiple C−S bonding, being significantly shorter than typical C−S single bonds (1.80−1.82 Å)[77] and comparable to η^2-CS_2 complex **8** (1.6986(14) Å). The C1−C2 bond length (1.338(7) Å) in complex **10** is akin to previously reported terminal mononuclear W-ketenylides.[3,5] Geometric constraints of chelation and pseudoolefinic coordination of the thioketene group result in a "bend-back" angle of 160.3(3)° at C1. The metric parameters associated with the η^2-(*S*,*C*)-S═C═C(^{t}Bu) moiety are remarkably similar to the corresponding values of the η^2-thioketenyl complex reported by Hill et al. in 1997 (Scheme 4C, above).[13]

Cyclic polymers are macrocyclic molecules with "ring-like" architectures with no chain ends. The lack of chain ends and topological constraints of their chain conformations result in unique physical characteristics compared to their linear counterparts with the same molecular weight, such as lower intrinsic viscosity,[78] smaller hydrodynamic volume,[79] lack of chain entanglement,[80] higher glass transition temperature (T_g),[81] higher brush density,[82] higher refractive index,[83,84] and increased rate of crystallization and nucleation density.[85] The exploration of cyclic polymers is not only limited to understanding their fundamental properties but also has emerging industrial interest in the materials science[86,87] and medical sectors.[88−90] One of the synthetic methods to access "ring-like" architecture is via ring expansion metathesis polymerization (REMP); the catalyst design involves tethering a metal−carbon double bond to generate a macrocyclic metal−alkylidene complex for the generation of cyclic polymers. Since 2002,[91] REMP research into new catalysts and cyclic polymers is rapidly growing.[3,5,10,16,18,92−94]

Both complexes **8** and **9** contain a tethered alkylidene moiety, but only complex **8** is an active initiator for norbornene polymerization via REMP. Treating **8** with norbornene in toluene at ambient temperature for 1 h yields *cis*-selective (>93% by ^{1}H NMR spectroscopy) *c*-poly(NBE) (Scheme 8). Adding the reaction mixture dropwise into a 10-fold excess of stirring methanol quenched the polymerization process and precipitated the polymer. Vacuum filtration followed by removal of all volatiles under vacuum overnight affords white *c*-poly(NBE). The M_n ranges between 10,000 and 24,000 g/mol and produces much lower-molecular-weight *cis*-syndiotactic *c*-poly(NBE) samples compared to complex **4-^{t}Bu**. The reason for the lower *cis*-selectivity and yield compared to **4-^{t}Bu** might be the formation of multiple products upon the dissociation of THF that occurs during the initial norbornene insertion at the W-center. Decreasing the monomer concentration from 0.25 to 0.1 M decreases the *cis*-selectivity and the yield of the resulting *c*-poly(NBE). However, wide variability in the M_n values of the resulting polymers limited any identification of specific trends.

The *c*-poly(NBE) produced with catalyst **8** is *cis* (>80%) and syndiotactic (>95%), as determined by comparing its ^{1}H and ^{13}C{^{1}H} NMR spectra to the previously reported syndiotactic linear polynorbornene (L-poly(NBE)).[4] Post-polymerization modification of norbornene via partial bromination of the double bonds generated two doublets at 3.84 (J = 9.9 Hz) and 3.80 (J = 9.5 Hz). Similar to the reported *cis*-syndiotactic L-poly(NBE), irradiating the methine proton at 2.61 ppm results in two singlets. In addition, the FTIR spectrum of *c*-poly(NBE) exhibits a strong IR absorption at 734 cm^{-1} (*cis*) and a relatively weak absorption at 956 cm^{-1} (*trans*).

Various measurements probing the hydrodynamic volume of the polymers provide evidence for a cyclic topology in the poly(NBE) synthesized by complex **8**, when compared to *cis*-syndiotactic L-poly(NBE). Mixing a solution of commercially available Grubbs catalyst[95] with norbornene in toluene produces the L-poly(NBE).[96] Figure 4 depicts the log of molar mass versus retention time of L-poly(NBE) and *c*-poly(NBE). Cyclic polymers possess smaller hydrodynamic volumes when compared to the same molar mass linear counterparts and therefore elute later. Figure 4 matches the prediction that cyclic structures elute later than linear polymers over a broad range of molar mass.

A Mark−Houwink−Sakurada (MHS) plot ([η] is the intrinsic viscosity, and M is the viscosity-average molar mass) also confirms a cyclic topology by demonstrating that cyclic polymers have lower intrinsic viscosities than the linear counterparts ($[\eta]_{cyclic} < [\eta]_{linear}$). Over a wide range of molecular weights, Figure 5 depicts the experimental ratio $[\eta]_{cyclic}/[\eta]_{linear}$ of 0.56 ± 0.20. The expected ratio range under θ conditions (a = 0.5) between 0.65[97,98] and 0.58 ± 0.01.[99] Experimental results are consistent, ranging from ∼0.4 to ∼0.8,[78,100−102] depending on the molecular weight[100,103] and the polymer−solvent system.[101,104]

https://doi.org/10.1021/acs.inorgchem.4c01522
Inorg. Chem. 2024, 63, 12207−12217

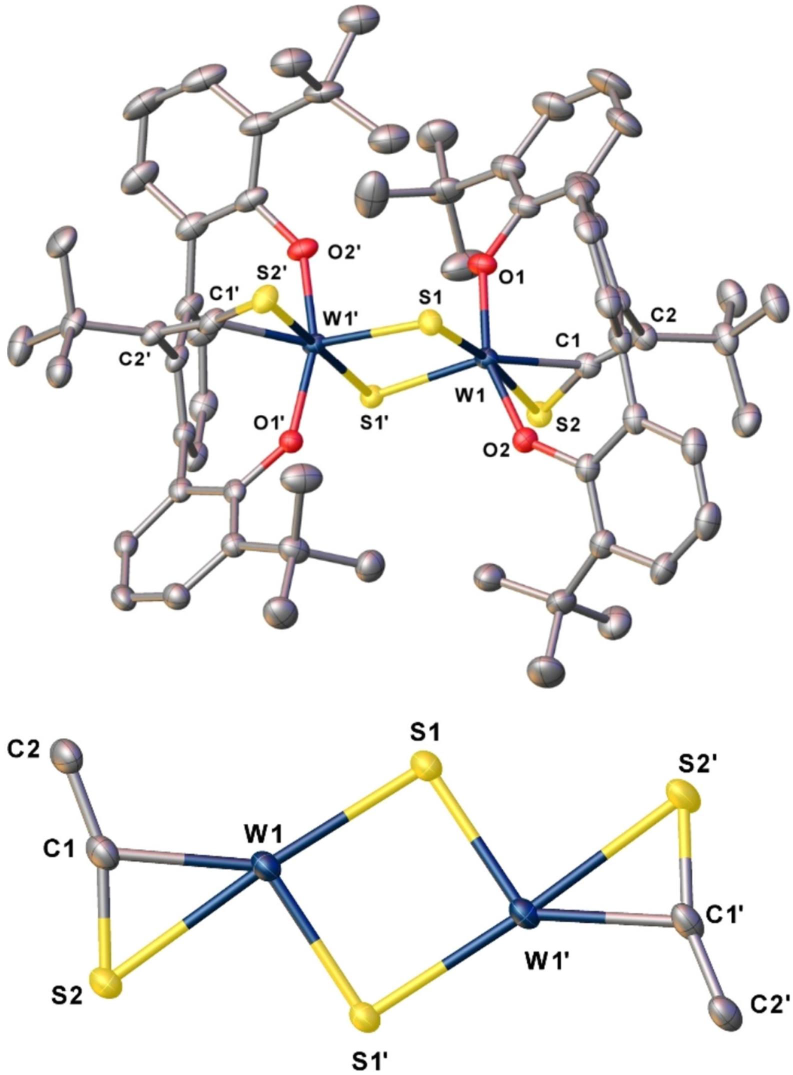

Figure 3. Solid-state molecular structure of **10** and truncated thermal ellipsoid plot (50% probability) of the W(VI) dimer core. Hydrogen and disordered atoms are removed for clarity. (Right): truncated thermal ellipsoid plot (50% probability) of the W(VI) dimer core. Selected bond distances [Å]: W1−C1 2.136(10), W1−S1 2.482(10), W1−S1′ 2.356(8), W1−S2 2.584(10), W1′-S1 2.349(8), W1′−S1′ 2.488(10), S2−C1 1.701(7), and C1−C2 1.338(7). Selected bond angles [°]: ∠W1−S1′-W1′ 90.5(3), ∠W1′−S1-W1 90.8(3), ∠S1−W1−S2 171.69(5), ∠C1−W1−S1 143.1(2), ∠C1−W1−S1′ 128.06(11), ∠C1−W1−S2 40.9(2), and ∠C2−C1−S2 160.3(3).

Scheme 8. Polymerization of Norbornene by Complex 8 to Generate *c*-poly(NBE)

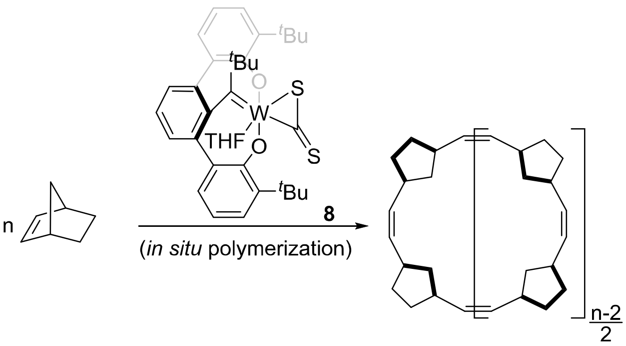

In addition, Figure 6 demonstrates the root-mean-square radius ($\langle R_g^2 \rangle$) versus the molecular weight of L-poly(NBE) versus c-poly(NBE). Cyclic and linear samples of the poly(NBE) demonstrate a $\langle R_g^2 \rangle_{cyclic} / \langle R_g^2 \rangle_{linear}$ ratio of 0.75 ± 0.09. The deviation mainly appears toward the edge of the overlapping regions of the molecular weights of the two samples, where the expected theoretical value is 0.5.[105]

■ CONCLUSIONS

By swapping the reaction between alkylidyne **1** and CO_2 with its heavier congener CS_2, the first tethered tungsten sulfido alkylidene complex was isolated and characterized. The chemistry is much different for CS_2 than for CO_2. For example, it is possible to isolate the η^2 bound CS_2 complex $[O_2C(^tBuC{=})W(\eta^2\text{-}(S,C)\text{-}CS_2)(THF)]$ **8**, whereas for CO_2, no intermediate is detectable or isolable prior to CO bond cleavage.

The role of THF as a coordinating solvent is once again highlighted in this system, where a loss of THF from the coordination sphere of complex **8** during solvent removal *in vacuo* generates multiple products and prevents isolation of **8** as a pure solid. Alternatively, the addition of THF converts **10** to **9**. THF coordination seems to play a central role in the

https://doi.org/10.1021/acs.inorgchem.4c01522
Inorg. Chem. 2024, 63, 12207−12217

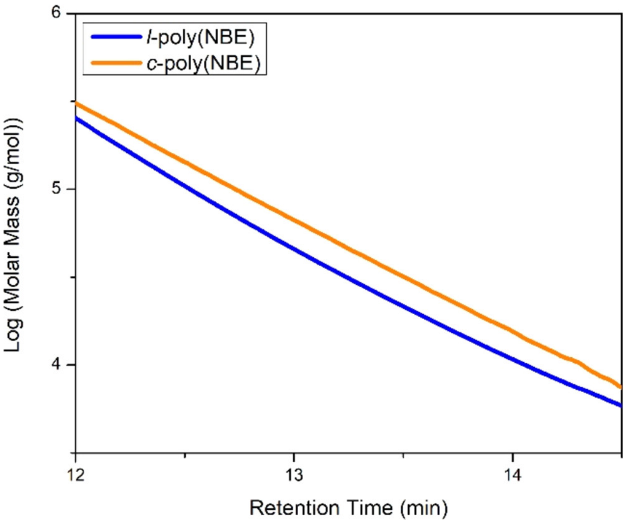

Figure 4. Log of molar mass versus retention time for L-poly(NBE) and *c*-poly(NBE) synthesized by complex **8**.

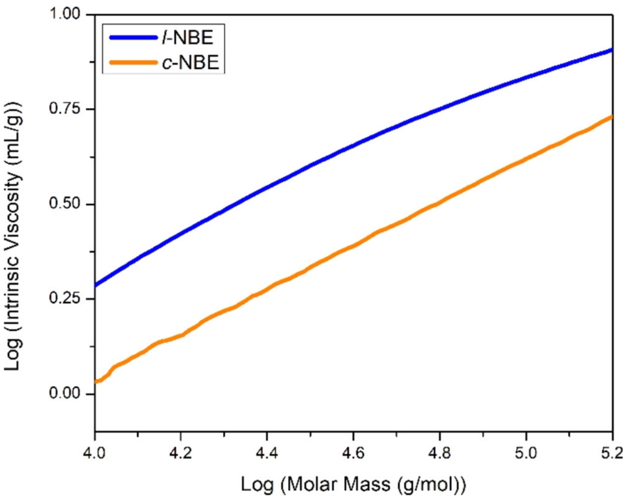

Figure 5. Log of [η] versus log of molar mass for L-poly(NBE) and *c*-poly(NBE) synthesized by complex **8**.

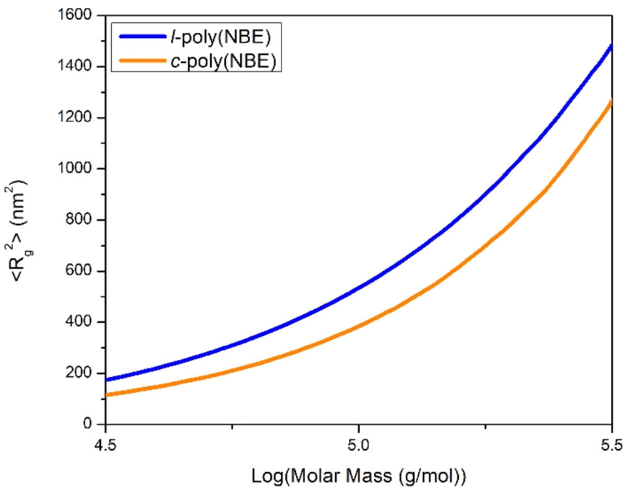

Figure 6. Plot of root-mean-square radius ($\langle R_g^2 \rangle$) versus log of molar mass for L-poly(NBE) and *c*-poly(NBE) synthesized by complex **8**.

pincer-tether C−C bond cleavage/formation. Previously, we discovered that rapid C−C bond cleavage occurs upon removal of THF *in vacuo* from the W-η^2-(R−N═C═O) and W-η^2-(R−C≡P) analogues of **8** to yield terminal ketenylide[5] and phosphametallacyclobutadiene[14] complexes, respectively.

Another stark difference is that C═O inserts into the tethered alkylidene linkage for CO_2, but for CS_2, the CS fragment is lost as insoluble $(CS)_x$. Also, compared to the tethered tungsten oxo alkylidene complex (**2**), complex **9** is more strained since it lacks the CS moiety in the tether. However, complex **9** does not initiate REMP. Despite both **8** and **9** containing a tethered alkylidene moiety, only complex **8** is an active REMP initiator. This information is critical, since it will inform future calculations that model the initiation mechanism. Any calculations will necessarily have to agree with the insurmountable activation barrier presented by **9**, a result we did not have prior to this work.

■ EXPERIMENTAL DETAILS

General Considerations. All manipulations were performed under an inert atmosphere using standard Schlenk or glovebox techniques. No uncommon hazards were noted. Glassware was oven-dried before use. Pentane, hexanes, toluene, diethyl ether (Et_2O), tetrahydrofuran (THF), benzene (C_6H_6), and toluene (C_7H_8) were dried using a Glass Contour drying column and stored over 3 Å molecular sieves. Toluene-d_8 (C_7D_8) and benzene-d_6 (C_6D_6) were purchased from Cambridge Isotope Laboratories and dried over calcium hydride (CaH_2) or with sodium-benzophenone under reflux conditions, distilled and degassed, and stored over 3 Å molecular sieves. Norbornene (NBE) was refluxed over sodium, distilled, and stored under nitrogen. The tungsten alkylidyne [^{t}BuOCO]W≡C^{t}Bu(THF)$_2$ (**1**)[1] was prepared according to published procedures. Linear *cis*-syndiotactic L-poly(NBE) was synthesized following a literature procedure,[96] using the commercially available Grubbs catalyst Ru(NHC(Ad)(Mes))(═CH(PhO^{i}Pr))-(η^2-NO_3)[95] and was purchased from Sigma-Aldrich (CAS Number 1352916-84-7) and used without purification. Post-polymerization bromination of poly(NBE) was conducted according to a literature procedure.[106] The ^{13}C-labeled carbon disulfide was purchased from Cambridge Isotope Laboratories and used as received.

^{1}H, ^{13}C{^{1}H}, and 2D NMR spectra were obtained on Varian INOVA (500 MHz) and Bruker (400 and 600 MHz) spectrometers. The chemical shifts are reported in δ (ppm) and are referenced to the lock signals on the TMS scale for ^{1}H and ^{13}C{^{1}H} spectra. The assignments are primarily based on the cross-peaks observed in the ^{1}H−^{13}C gHMBC and gHSQC spectra. The spectra were recorded at 25 °C unless noted otherwise.

Fourier transform infrared (FTIR) spectra were collected on drop-cast samples using a Thermo Fisher Scientific Nicolet iS5 spectrometer equipped with an iD7 ATR stage and using the OMNIC software package at 1.0 cm^{-1} resolution and 32 scans per sample. FTIR spectra were recorded as solids on a Thermo Nicolet 5700 FTIR spectrometer equipped with a single bounce, diamond-stage attenuated total reflectance (ATR) accessory.

Electrospray ionization mass spectrometry (ESI-MS) spectra were collected by direct injection into an Agilent 6120 time-of-flight (TOF) spectrometer at a gas temperature of 350 °C with a fragmentation voltage of 120 V. Solution samples were prepared in anhydrous THF and loaded into Hamilton Gastight SampleLock syringes inside a nitrogen-filled glovebox.

Polymer samples were analyzed by size-exclusion chromatography in THF at 35 °C and a flow rate of 1.0 mL/min (Agilent isocratic pump, degasser, and autosampler; columns: three PLgel 5 μm MIXED-D mixed bed columns, molecular weight range 200−400,000 g/mol). Detection consisted of a Wyatt Optilab rEX refractive index detector operating at 658 nm, a Wyatt miniDAWN Treos light scattering detector operating at 656 nm, and a Wyatt ViscoStar-II

https://doi.org/10.1021/acs.inorgchem.4c01522
Inorg. Chem. 2024, 63, 12207−12217

viscometer. Absolute molecular weights and molecular weight distributions were calculated using Wyatt ASTRA software.

■ ASSOCIATED CONTENT

Supporting Information

The Supporting Information is available free of charge at https://pubs.acs.org/doi/10.1021/acs.inorgchem.4c01522.

Full experimental procedures, NMR spectra, and X-ray crystallographic and GC/EI-MS data. (PDF)

Accession Codes

CCDC 2350969–2350971 contain the supplementary crystallographic data for this paper. These data can be obtained free of charge via www.ccdc.cam.ac.uk/data_request/cif, by emailing data_request@ccdc.cam.ac.uk, or by contacting The Cambridge Crystallographic Data Centre, 12 Union Road, Cambridge CB2 1EZ, UK; fax: +44 1223 336033.

■ AUTHOR INFORMATION

Corresponding Author

Adam S. Veige – *Department of Chemistry, Center for Catalysis, University of Florida, Gainesville, Florida 32611, United States;* orcid.org/0000-0002-7020-9251; Email: veige@chem.ufl.edu

Authors

Vineet K. Jakhar – *Department of Chemistry, Center for Catalysis, University of Florida, Gainesville, Florida 32611, United States;* orcid.org/0009-0003-3846-2286

Yu-Hsuan Shen – *Department of Chemistry, Center for Catalysis, University of Florida, Gainesville, Florida 32611, United States;* orcid.org/0000-0003-0976-4034

Rinku Yadav – *Department of Chemistry, Center for Catalysis, University of Florida, Gainesville, Florida 32611, United States*

Soufiane S. Nadif – *Department of Chemistry, Center for Catalysis, University of Florida, Gainesville, Florida 32611, United States*

Ion Ghiviriga – *Department of Chemistry, Center for Catalysis, University of Florida, Gainesville, Florida 32611, United States;* orcid.org/0000-0001-5812-5170

Khalil A. Abboud – *Department of Chemistry, Center for Catalysis, University of Florida, Gainesville, Florida 32611, United States*

Daniel W. Lester – *Polymer Characterization Research Technology Platform, University of Warwick, Coventry CV4 7AL, United Kingdom*

Complete contact information is available at: https://pubs.acs.org/10.1021/acs.inorgchem.4c01522

Author Contributions

The manuscript was written through contributions of all authors. All authors have given approval to the final version of the manuscript.

Notes

The authors declare the following competing financial interest(s): ASV has an equity stake in a company (Oboro Labs) that involves the marketing of cyclic polymers and catalysts. ASV, VKJ, RY and UF have filed provisional patents on this subject matter.

■ ACKNOWLEDGMENTS

This material is based upon work supported by the National Science Foundation CHE-2154377 (A.S.V.). The GC/EI-MS instrument is funded by NIH S10 OD021758-01A1. K.A.A. acknowledges the NSF (CHE-1828064) and UF for the purchase of X-ray equipment.

■ REFERENCES

(1) Sarkar, S.; McGowan, K. P.; Kuppuswamy, S.; Ghiviriga, I.; Abboud, K. A.; Veige, A. S. An OCO^{3-} Trianionic Pincer Tungsten(VI) Alkylidyne: Rational Design of a Highly Active Alkyne Polymerization Catalyst. *J. Am. Chem. Soc.* **2012**, *134* (10), 4509–4512.

(2) Kuppuswamy, S.; Peloquin, A. J.; Ghiviriga, I.; Abboud, K. A.; Veige, A. S. Synthesis and Characterization of Tungsten(VI) Alkylidene Complexes Supported by an $[OCO]^{3-}$ Trianionic Pincer Ligand: Progress towards the $[^{t}BuOCO]W{\equiv}CC(CH_3)_3$ Fragment. *Organometallics* **2010**, *29* (19), 4227–4233.

(3) Gonsales, S. A.; Kubo, T.; Flint, M. K.; Abboud, K. A.; Sumerlin, B. S.; Veige, A. S. Highly Tactic Cyclic Polynorbornene: Stereoselective Ring Expansion Metathesis Polymerization of Norbornene Catalyzed by a New Tethered Tungsten-Alkylidene Catalyst. *J. Am. Chem. Soc.* **2016**, *138* (15), 4996–4999.

(4) Hyun, S.-M.; Marathianos, A.; Boeck, P. T.; Ghiviriga, I.; Lester, D. W.; Sumerlin, B. S.; Veige, A. S. Influence of Solvent on Cyclic Polynorbornene Tacticity. *Chem. Commun.* **2023**, *59*, 13993–13996.

(5) Jakhar, V.; Pal, D.; Ghiviriga, I.; Abboud, K. A.; Lester, D. W.; Sumerlin, B. S.; Veige, A. S. Tethered Tungsten-Alkylidenes for the Synthesis of Cyclic Polynorbornene via Ring Expansion Metathesis: Unprecedented Stereoselectivity and Trapping of Key Catalytic Intermediates. *J. Am. Chem. Soc.* **2021**, *143* (2), 1235–1246.

(6) Probst, P.; Groos, J.; Wang, D.; Beck, A.; Gugeler, K.; Kästner, J.; Frey, W.; Buchmeiser, M. R. Stereoselective Ring Expansion Metathesis Polymerization with Cationic Molybdenum Alkylidyne N-Heterocyclic Carbene Complexes. *J. Am. Chem. Soc.* **2024**, *146* (12), 8435–8446.

(7) Morrison, C. M.; Golder, M. R. Ring-Expansion Metathesis Polymerization Initiator Design for the Synthesis of Cyclic Polymers. *Synlett* **2022**, *33* (8), 699–704.

(8) Wang, T. W.; Huang, P. R.; Chow, J. L.; Kaminsky, W.; Golder, M. R. A Cyclic Ruthenium Benzylidene Initiator Platform Enhances Reactivity for Ring-Expansion Metathesis Polymerization. *J. Am. Chem. Soc.* **2021**, *143* (19), 7314–7319.

(9) Wang, T. W.; Golder, M. R. Advancing Macromolecular Hoop Construction: Recent Developments in Synthetic Cyclic Polymer Chemistry. *Polym. Chem.* **2021**, *12* (7), 958–969.

(10) Yadav, R.; Esper, A. M.; Ghiviriga, I.; Abboud, K. A.; Lester, W.; Ehm, C.; Veige, A. S. REMP Initiators with an Unusual Ancillary Ligand. *ChemCatChem* **2023**, No. e202301678, DOI: 10.1002/cctc.202301678.

(11) Mayr, A.; Lee, T.-Y. Formation of Alkynyltrithiocarbonato Ligands from Alkylidyne Ligands and Carbon Disulfide. *Angew. Chem., Int. Ed.* **1993**, *32* (12), 1726–1727.

(12) Bedford, R. B.; Hill, A. F.; White, A. J. P.; Williams, D. J. Cycloadditions of Ruthenium Alkylidyne Complexes with Carbonyl or Thiocarbonyl Compounds. *Angew. Chem,. Int. Ed.* **1996**, *35* (1), 95–97.

(13) Hill, A. F.; Malget, J. M.; White, A. J. P.; Williams, D. J. A Thioketene Complex of Molybdenum(IV): Crystal Structure of $[Mo\{\eta^2\text{-K}(C,S),\sigma\text{-K}(S')\text{-}$ SdCdCRC(DO)S}(DO){HB(Pz)$_3$}](R) C_6H_4Me-4, Pz) Pyrazol-1-Yl). *Inorg. Chem.* **1998**, *37* (3), 598–600.

(14) Jakhar, V. K.; Esper, A. M.; Ghiviriga, I.; Abboud, K. A.; Ehm, C.; Veige, A. S. Isolation of an Elusive Phosphametallacyclobutadiene and Its Role in Reversible Carbon–Carbon Bond Cleavage. *Angew. Chem., Int. Ed.* **2022**, *61* (30), No. e202203073.

(15) Miao, Z.; Konar, D.; Sumerlin, B. S.; Veige, A. S. Soluble Polymer Precursors via Ring-Expansion Metathesis Polymerization for

the Synthesis of Cyclic Polyacetylene. *Macromolecules* **2021**, *54* (17), 7840−7848.
(16) Nadif, S. S.; Kubo, T.; Gonsales, S. A.; Venkatramani, S.; Ghiviriga, I.; Sumerlin, B. S.; Veige, A. S. Introducing "Ynene" Metathesis: Ring-Expansion Metathesis Polymerization Leads to Highly Cis and Syndiotactic Cyclic Polymers of Norbornene. *J. Am. Chem. Soc.* **2016**, *138* (20), 6408−6411.
(17) Mcgowan, K. P.; O'Reilly, M. E.; Ghiviriga, I.; Abboud, K. A.; Veige, A. S. Compelling Mechanistic Data and Identification of the Active Species in Tungsten-Catalyzed Alkyne Polymerizations: Conversion of a Trianionic Pincer into a New Tetraanionic Pincer-Type Ligand. *Chem. Sci.* **2013**, *4* (3), 1145−1155.
(18) Roland, C. D.; Li, H.; Abboud, K. A.; Wagener, K. B.; Veige, A. S. Cyclic Polymers from Alkynes. *Nat. Chem.* **2016**, *8* (8), 791−796.
(19) Roland, C. D.; Zhang, T.; Venkatramani, S.; Ghiviriga, I.; Veige, A. S. A Catalytically Relevant Intermediate in the Synthesis of Cyclic Polymers from Alkynes. *Chem. Commun.* **2019**, *55* (91), 13697−13700.
(20) Kleman, B. The Near-Ultraviolet Absorption Spectrum of CS_2. *Can. J. Phys.* **1963**, *41* (7723), 2034−2063.
(21) Bianchini, C.; Masi, D.; Mealli, C.; Meli, A.; Sabat, M. Effects of the Conformational Rearrangement of the $(Np_3)M$ Fragment in the Course of the Reaction between $(Np_3)MH$ Hydrides [M = Co, Rh; Np_3 = $N(CH_2CH_2PPh_2)_3$] and Carbon Disulfide. *Organometallics* **1985**, *4* (6), 1014−1019.
(22) Lindner, E.; Keppeler, B.; Mayer, H. A.; Gierling, K.; Fawzi, R.; Steimann, M. Substrate Activation by the Wilkinson Analogous Complex ClRh(P ∼ O)(P O) Containing η^2-PO-Chelated and η^1-P-Bonded (Methoxyethyl) Dicyclohexylphosphine as a Hemilabile Ligand. *J. Organomet. Chem.* **1996**, *526* (1), 175−183.
(23) Doux, M.; Mézailles, N.; Ricard, L.; Le Floch, P. Planar Discrimination in an SPS-Based Rhodium(I) Complex. *Organometallics* **2003**, *22* (23), 4624−4626.
(24) Bheemaraju, A.; Beattie, J. W.; Lord, R. L.; Martin, P. D.; Groysman, S. Carbon Disulfide Binding at Dinuclear and Mononuclear Nickel Complexes Ligated by a Redox-Active Ligand: Iminopyridine Serving as an Accumulator of Redox Equivalents for the Activation of Heteroallenes. *Chem. Commun.* **2012**, *48* (77), 9595−9597.
(25) Bheemaraju, A.; Beattie, J. W.; Tabasan, E. G.; Martin, P. D.; Lord, R. L.; Groysman, S. Steric and Electronic Effects in the Formation and Carbon Disulfide Reactivity of Dinuclear Nickel Complexes Supported by Bis(Iminopyridine) Ligands. *Organometallics* **2013**, *32* (10), 2952−2962.
(26) Zheng, T.; Xu, W.; Li, J.; Lu, F. Crystal Structure of (2,3,6,7-Tetrahydro-1,3,7-Trimethyl-2,6-Dioxo-1Hpurin-8-Yl-KC)(Di-Thiocarboxylato-2-K2C,S)-tris(trimethylphosphine-KP) Cobalt(I) Tetrahydrofuran Solvate. *Z. Kristallogr.* **2013**, *228* (2), 189−190.
(27) Kläring, P.; Braun, T. Insertion of CS_2 into Iridium-Fluorine Bonds. *Angew. Chem., Int. Ed.* **2013**, *52* (42), 11096−11101.
(28) Dorta, R.; Linden, A.; Llovera, L.; Herrera, J.; Dorta, R.; Agrifoglio, G. Chiral-at-Metal" Hemilabile Nickel Complexes with a Latent d^{10}-ML_2 Configuration: Receiving Substrates with Open Arms. *Organometallics* **2012**, *31* (17), 6162−6171.
(29) Huang, N.; Li, X.; Xu, W.; Sun, H. Nickel-Heterocumulene Complexes Stabilized by Trimethylphosphine: Synthesis, Characterization and Catalytic Application in Organozinc Coupling with CS_2. *Inorg. Chim. Acta* **2013**, *394*, 446−451.
(30) Kashiwagi, T.; Yasuoka, N.; Ueki, T.; Kasai, N.; Kakudo, M.; et al. Addition of Some Simple Molecules to Transition Metal-Phosphine Complex and the Crystal and Molecular Structure of $Pd\{(C_6H_5)_3P\}_2(CS_2)$. *Bull. Chem. Soc. Jpn.* **1968**, *41*, 296−303.
(31) Schenk, W. A.; Kuemmerle, D.; Burschka, C. Die Koordinationschemie CS-Funktioneller Verbindungen. VIII. Addition Aktivierter Alkine an Wolfram-CS_2-Komplexe Und Aufbau Tetraedrischer Methylidindicobaitwolfram-Cluster. *J. Organomet. Chem.* **1988**, *349* (1−2), 183−196.
(32) Schenk, W. A.; Schwietzke, T.; Müller, H. Reaktivität von Wolfram-CS_2-Komplexen. *J. Organomet. Chem.* **1982**, *232* (1), C41−C47.
(33) Schenk, W. A.; Kuemmerle, D.; Schwietzke, T. Die Koordinationschemie CS-Funktioneller Verbindungen. VII. Elektrophiler Und Nukleophiler Angriff an Wolfram-CS2-Komplexen. *J. Organomet. Chem.* **1988**, *349* (1−2), 163−181.
(34) Roland, C. D.; Venkatramani, S.; Jakhar, V. K.; Ghiviriga, I.; Abboud, K. A.; Veige, A. S. Synthesis and Characterization of a Molybdenum Alkylidyne Supported by a Trianionic OCO^{3-} Pincer Ligand. *Organometallics* **2018**, *37* (23), 4500−4505.
(35) Nau, W. M.; Bucher, G.; Scaiano, J. C. Absolute Rate Constants for the Reactions of Sulfur (^3P_J) Atoms in Solution. *J. Am. Chem. Soc.* **1997**, *119* (8), 1961−1970.
(36) Liu, Y. S.; Bei, M. Z.; Zhou, Z. H.; Takaki, K.; Fujiwara, Y. SmI_2 Promoted Coupling Reaction of Isocyanates to Oxamides. *Chem. Lett.* **1992**, *21* (7), 1143−1144.
(37) Ley, S. V.; Taylor, S. J. A Polymer-Supported [1,3,2]-Oxazaphospholidine for the Conversion of Isothiocyanates to Isocyanides and Their Subsequent Use in an Ugi Reaction. *Bioorg. Med. Chem. Lett.* **2002**, *12* (14), 1813−1816.
(38) Addison, A. W.; Rao, T. N.; Reedijk, J.; Van Rijn, J.; Verschoor, G. C. Synthesis, Structure, and Spectroscopic Properties of Copper(II) Compounds Containing Nitrogen-Sulphur Donor Ligands; the Crystal and Molecular Structure of Aqua[1,7-Bis(N-Methylbenzimidazol-2′;-Yl)-2,6-Dithiaheptane]Copper(II) Perchlorate. *J. Chem. Soc., Dalton Trans.* **1984**, *0* (7), 1349−1356.
(39) Yadav, R.; Ghiviriga, I.; Abboud, K. K.; Veige, A. S. A Case of Alkylidyne-Imine Metathesis. *Chem. Commun.* **2023**, *59* (86), 12899−12902.
(40) Hauser, P. M.; Gugeler, K.; Frey, W.; Kästner, J.; Buchmeiser, M. R. Tungsten Sulfido Alkylidene and Cationic Tungsten Sulfido Alkylidene N-Heterocyclic Carbene Complexes. *Organometallics* **2021**, *40* (23), 4026−4034.
(41) Chisholm, M. H.; Huffman, J. C.; Pasterczyk, J. W. Synthesis and Reactivity of Compounds of Formula $W(S)(OR)_4$. *Polyhedron* **1987**, *6* (7), 1551−1557.
(42) Rabinovich, D.; Parkin, G. The Syntheses, Structures, and Reactivity of Monomeric Tungsten(IV) and Tungsten(VI)bis-(Sulfido) Complexes: Facile Elimination of H_2 from H_2S. *J. Am. Chem. Soc.* **1991**, *113*, 5904−5905.
(43) Klabunde, K. J.; Moltzen, E.; Voska, K. Carbon Monosulfide Chemistry. Reactivity and Polymerization Studies. *Phosphorus Sulfur Silicon Relat. Elem.* **1989**, *43* (1−2), 47−61.
(44) Ahrens, T.; Schmiedecke, B.; Braun, T.; Herrmann, R.; Laubenstein, R. Activation of CS_2 and COS at a Rhodium(I) Germyl Complex: Generation of CS and Carbido Complexes. *Eur. J. Inorg. Chem.* **2017**, *2017* (3), 713−722.
(45) Trnka, T. M.; Parkin, G. A Survey of Terminal Chalcogenido Complexes of the Transition Metals : Trends in Their Distribution and the Variation of Their M = E Bond Lengths. *Polyhedron* **1997**, *16* (7), 1031−1045.
(46) Parkin, G. *Terminal Chalcogenido Complexes of the Transition Metals*; Wiley, 1998; Vol. *47*.
(47) Bhaduri, S.; Ibers, J. A. Synthesis of the Octathiotritungstate Anion, $[W_3S_8]^{2-}$. First Example of Square-Planar Coordination about a Tungsten Atom. *Inorg. Chem.* **1986**, *25* (1), 3−4.
(48) Secheresse, F.; Lavigne, G.; Jeannin, Y.; Lefebvre, J. Synthesis and Molecular Structure of Bis(Tetrathiotungstato(VI)-S,S')-Oxotungstate(IV), $(C_6H_5)_4P)_2(WO(WS_4)_2)^{-2})$. *J. Coord. Chem.* **1981**, *11* (1), 11−16.
(49) Secheresse, F.; Lefebvre, J.; Daran, J. C.; Jeannin, Y. Synthesis and Structure of the First Tungsten Complex Having the $(W_2S_4)^{2+}$ Core: $[P(C_6H_5)_4]_2W_4S_{12}$. *Inorg. Chem.* **1982**, *21* (4), 1311−1314.
(50) Pan, W.; Chandler, T.; Enemark, J. H.; Stiefel, E. I. Reactions of Tetrathiometalates, $(MS_4)^{2-}$ (M = Mo, W). Syntheses and Properties of $(M_2S_4)^{2+}$ Containing Compounds. Structure of Bis-(Tetraphenylphosphonium) Bis(M-Sulfido)Bis(Sulfido(1,2-

Ethanedithiolato)Tungstate(V)), $[P(C_6H_5)_4]_2[W_2S_4(S_2C_2H_4)_2]$. *Inorg. Chem.* **1984**, *23*, 4265−4269.

(51) Drew, M. G. B.; Hobson, R. J.; Mumba, P. P. E. M.; Rice, D. A.; Turp, N. Dimeric Tungsten(V) Compounds Containing $[(S)W(\mu\text{-}S)_2W(S)]^{2+}$. Syntheses and Structures of Di-μ-Sul Phido-Bis[(Diethyl Dithiophosphato-SS')SuIphido-Tungsten(V)] and Di-μ-Sulphido-Bis-[(N,N-Diethyldithiocarbamato-SS')- SuIph Idotungsten(V)]. *J. Chem. Soc., Dalton Trans.* **1987**, 1163−1167.

(52) Muller, A.; Diemann, E.; Wienboker, U.; Bogge, H. Formation of the Metal-Sulfide Aggregate $[W_3S_{10}]^{2-}$ through a Novel Balanced Intramolecular Condensation Redox Process with Principal Relevance to the Formation of Amorphous Metal Sulfides like WS_3. *Inorg. Chem.* **1989**, *495* (1), 4046−4049.

(53) Cohen, S. A.; Stiefel, E. I. Dinuclear Tungsten(V) and Molybdenum(V) Compounds Containing $M_2S_2(\mu\text{-}S_2)^{2+}$ Cores. Synthesis and Reactivity of $[N(C_2H_5)_4]_2M_2S_{12}$ (M = W or Mo) and the Crystal Structure of $[N(C_2H_5)_4]_2W_2S_2(\mu\text{-}S)_2(S_4)_2$. *Inorg. Chem.* **1985**, *24*, 4657−4662.

(54) Simonnet-jegat, C.; Toscano, A.; Robert, F.; Darana, J.; S, F. S. Acidification of $[WS_4]^{2-}$. Synthesis and Structures of Di-μ-Sulfido-Bis[(2,2′-Bipyridine)Chlorooxotungsten(V)] and Di-μ-Sulfido-Bis-[(2,2′-Bipyridine)Bromooxotungsten(V)]. *J. Chem. Soc., Dalton Trans.* **1994**, *8*, 1311−1315.

(55) Mukherjee, A. K.; Das, P. K.; Mukherjee, M.; Chakraborty, P. K.; Bhattacharya, R. Disorder in Bis(Tetraethylammonium) Bis(μ-Sulfido)Bis[(1,2,3,4-Tetrathiabutane-1,4-Diyl-S,S)Thiotungstate(V)]. *Acta Crystallogr., Sect. C* **1997**, *53*, 209−212.

(56) Mallard, A.; Simonnet-Jégat, C.; Lavanant, H.; Marrot, J.; Sécheresse, F. Reactivity of Tetrathiometalates with Alkynes. Synthesis and Characterisation of Dithiolene Complexes of Mo, W, and V by ESMS and XRD. *Trans. Met. Chem.* **2008**, *33* (2), 143−152.

(57) Ward, J. P.; Lim, P. J.; Evans, D. J.; White, J. M.; Young, C. G. Tungsten Ligand-Based Sulfur-Atom-Transfer Catalysts: Synthesis, Characterization, Sustained Anaerobic Catalysis, and Mode of Aerial Deactivation. *Inorg. Chem.* **2020**, *59* (23), 16824−16828.

(58) Goddard, C. A.; Holm, R. H. Synthesis and Reactivity Aspects of the Bis(Dithiolene) Chalcogenide Series $[WIVQ(S_2C_2R_2)_2]^{2-}$ (Q = O, S, Se). *Inorg. Chem.* **1999**, *38* (23), 5389−5398.

(59) Umakoshi, K.; Nishimoto, E.; Sokolov, M.; Kawano, H.; Sasaki, Y.; Onishi, M. Synthesis, Structure, and Properties of Sulfido-Bridged Dinuclear Tungsten(V) Complex of Dithiolene, $(Pr_4N)_2[W_2(\mu\text{-}S)_2\{S_2C_2(CO_2Et)_2\}_4]$. *J. Organomet. Chem.* **2000**, *611* (1−2), 370−375.

(60) Sung, K. M.; Holm, R. H. Substitution and Oxidation Reactions of Bis(Dithiolene)Tungsten Complexes of Potential Relevance to Enzyme Sites. *Inorg. Chem.* **2001**, *40* (18), 4518−4525.

(61) Seino, H.; Iwata, N.; Kawarai, N.; Hidai, M.; Mizobe, Y. A Series of Dinuclear Homo- and Heterometallic Complexes with Two or Three Bridging Sulfido Ligands Derived from the Tungsten Tris(Sulfido) Complex $[Et_4N][(Me_2Tp)WS_3]$ (Me_2Tp = Hydridotris(3,5-Dimethylpyrazol-1-Yl)Borate). *Inorg. Chem.* **2003**, *42* (23), 7387−7395.

(62) Weiss, K.; Schubert, U.; Schrock, R. R. Metathesis-Like Reaction of a Tungsten Alkylidyne Complex with Cyclohexyl Isocyanate. *Organometallics* **1986**, *5*, 397−398.

(63) Neithamer, D. R.; LaPointe, R. E.; Wheeler, R. A.; Richeson, D. S.; Duyne, G. D.; Van; Wolczanski, P. T. Carbon Monoxide Cleavage by $(Silox)_3Ta$ (Silox = $^tBu_3SiO$-): Physical, Theoretical, and Mechanistic Investigations. *J. Am. Chem. Soc.* **1989**, *111*, 9056−9072.

(64) List, A. K.; Hillhouse, G. L.; Rheingold, A. L. Carbon Suboxide as a C1 Reagent. Sequential Cleavage of CO from C_3O_2 at a Metal Center to Give $WCl_2(CO)(PMePh_2)_2\{C, C':\eta^2\text{-}C(O)CPMePh_2)$ and $WCl_2(CO)(PMePh_2)_2(=CPMePh_2)$. *Organometallics* **1989**, *8* (8), 2010−2016.

(65) Jensen, M. P.; Shriver, D. F. CC and CO Transformations in Ketenylidene Cluster Compounds. *J. Mol. Catal.* **1992**, *74* (1−3), 73−84.

(66) Jensen, M. P.; Phillips, D. A.; Sabat, M.; Shriver, D. F. Cluster-Bound Ketenylidenes as Precursors to Dicarbide Ligands: Synthesis and Characterization of $[PPN][Fe_3CO_3(C_2)(CO)_{18}]$. *Organometallics* **1992**, *11* (5), 1859−1869.

(67) Johnston, D. H.; Stern, C. L.; Shriver, D. F. Synthesis of Heterometallic Butterfly Carbide Clusters Containing Three Different Metals: $(PPN)[Fe_2CoM(Dmpm)(CO)_{11}C]$ (MMo or W). *Inorg. Chim. Acta* **1993**, *213* (1−2), 83−90.

(68) Norton, D. M.; Stern, C. L.; Shriver, D. F. A New Route to a C4 Ligand: Carbon-Carbon Coupling To Generate $[PPN]_2[Fe_6(CO)I_8C_4$. *Inorg. Chem.* **1994**, *33* (13), 2701−2702.

(69) Wong, W.-Y.; Wong, W.-T. Synthesis and Structural Characterisation of Some New Triosmium Alkylidyne Clusters Containing Sulfur-Donor Ligands. The Formation of C-S and C-C Bonds. *J. Chem. Soc., Dalton Trans.* **1995**, *17*, 2735−2740.

(70) Eveland, R. W.; Raymond, C. C.; Albrecht-Schmitt, T. E.; Shriver, D. F. New SO_2 Iron-Containing Cluster Compounds $[PPN]_2[Fe_3(CO)_9(M_3,\eta^2\text{-}SO_2)]$, $[PPN]_2[Fe_3(CO)_8(\mu\text{-}SO_2)\mu^3\text{-}S]$, $[PPN]_2[Fe_3(CO)_8(\mu\text{-}SO_2)(M_3\text{-}CCO)]$, and $[PPN]_2[Fe_2(CO)_6(\mu\text{-}SO_2)=]$ from Heterometal Precursors. *Inorg. Chem.* **1999**, *38*, 1282−1287.

(71) Norton, D. M.; Shriver, D. F. Synthesis and Characterization of a Polycarbon Organometallic Cluster, $[PPN]_2[Fe_6(CO)_{18}C_4]$. *Inorg. Chem.* **2000**, *39* (22), 5118−5120.

(72) Wells, K. D.; McDonald, R.; Ferguson, M. J.; Cowie, M. Unusual Ligand Transformations Initiated by Dppm Deprotonation in Methylene-Bridged Rh/Os Complexes. *Inorg. Chem.* **2011**, *50* (8), 3523−3538.

(73) Xiao, F. S.; Ichikawa, M. Oxide-Supported Triruthenium Ketenylidene Clusters and Their Catalytic Properties. *J. Mol. Catal., A* **1996**, *113* (3), 427−444.

(74) Thöne, C.; Vahrenkamp, H. Aurated Clusters Derived from (μ^3-Ketenylidene)-Fe_3 and -Fe_2Co Clusters. *J. Organomet. Chem.* **1995**, *485* (1−2), 185−189.

(75) Caldwell, L. M.; Hill, A. F.; Stranger, R.; Terrett, R. N. L.; Nessi, K. M.; von Ward, J. S.; Willis, A. C. Thioxoethenylidene (CCS) as a Bridging Ligand. *Organometallics* **2015**, *34* (1), 328−334.

(76) Antoni, P. W.; Reitz, J.; Hansmann, M. M. N2/CO Exchange at a Vinylidene Carbon Center: Stable Alkylidene Ketenes and Alkylidene Thioketenes from 1,2,3-Triazole Derived Diazoalkenes. *J. Am. Chem. Soc.* **2021**, *143* (32), 12878−12885.

(77) Oae, S.; Kunieda, N.Sulfinic Acids and Sulfinic Esters. In *Organic Chemistry of Sulfur*; Wiley, 1977; pp 603−647.

(78) Jeong, Y.; Jin, Y.; Chang, T.; Uhlik, F.; Roovers, J. Intrinsic Viscosity of Cyclic Polystyrene. *Macromolecules* **2017**, *50* (19), 7770−7776.

(79) Dodgson, K.; Sympson, D.; Semlyen, J. A. Studies of Cyclic and Linear Poly(Dimethyl Siloxanes): 2. Preparative Gel Permeation Chromatography. *Polymer* **1978**, *19* (11), 1285−1289.

(80) Jia, Z.; Monteiro, M. J. Cyclic Polymers: Methods and Strategies. *J. Polym. Sci., Part A: Polym. Chem.* **2012**, *50* (11), 2085−2097.

(81) Clarson, S. J.; Dodgson, K.; Semlyen, J. A. Studies of Cyclic and Linear Poly(Dimethylsiloxanes): 19. Glass Transition Temperatures and Crystallization Behaviour. *Polymer* **1985**, *26* (6), 930−934.

(82) Morgese, G.; Trachsel, L.; Romio, M.; Divandari, M.; Ramakrishna, S. N.; Benetti, E. M. Topological Polymer Chemistry Enters Surface Science: Linear versus Cyclic Polymer Brushes. *Angew. Chem., Int. Ed.* **2016**, *55* (50), 15583−15588.

(83) Bannister, D. J.; Semlyen, J. A. Studies of Cyclic and Linear Poly(Dimethyl Siloxanes): 6. Effect of Heat. *Polymer* **1981**, *22* (3), 377−381.

(84) Orrah, D. J.; Semlyen, J. A.; Ross-Murphy, S. B. Studies of Cyclic and Linear Poly(Dimethylsiloxanes): 28. Viscosities and Densities of Ring and Chain Poly(Dimethylsiloxane) Blends. *Polymer* **1988**, *29* (8), 1455−1458.

(85) Zaldua, N.; Liénard, R.; Josse, T.; Zubitur, M.; Mugica, A.; Iturrospe, A.; Arbe, A.; De Winter, J.; Coulembier, O.; Müller, A. J. Influence of Chain Topology (Cyclic versus Linear) on the Nucleation and Isothermal Crystallization of Poly(l -Lactide) and Poly(d -Lactide). *Macromolecules* **2018**, *51* (5), 1718−1732.

(86) Tuba, R. Synthesis of Cyclopolyolefins via Ruthenium Catalyzed Ring-Expansion Metathesis Polymerization. *Pure Appl. Chem.* **2014**, *86* (11), 1685−1693.
(87) Zhu, Y.; Hosmane, N. S. Advanced Developments in Cyclic Polymers: Synthesis, Applications, and Perspectives. *ChemistryOpen* **2015**, *4* (4), 408−417.
(88) Tu, X. Y.; Liu, M. Z.; Wei, H. Recent Progress on Cyclic Polymers: Synthesis, Bioproperties, and Biomedical Applications. *J. Polym. Sci., Part A: Polym. Chem.* **2016**, *54* (11), 1447−1458.
(89) Haque, F. M.; Grayson, S. M. The Synthesis, Properties and Potential Applications of Cyclic Polymers. *Nat. Chem.* **2020**, *12* (5), 433−444.
(90) Liénard, R.; De Winter, J.; Coulembier, O. Cyclic Polymers: Advances in Their Synthesis, Properties, and Biomedical Applications. *J. Polym. Sci.* **2020**, *58* (11), 1481−1502.
(91) Bielawski, C. W.; Benitez, D.; Grubbs, R. H. An "Endless" Route to Cyclic Polymers. *Science* **2002**, *297* (5589), 2041−2044.
(92) Yoon, K. Y.; Noh, J.; Gan, Q.; Edwards, J. P.; Tuba, R.; Choi, T. L.; Grubbs, R. H. Scalable and Continuous Access to Pure Cyclic Polymers Enabled by 'Quarantined' Heterogeneous Catalysts. *Nat. Chem.* **2022**, *14* (5), 1242−1248.
(93) Boydston, A. J.; Xia, Y.; Kornfield, J. A.; Gorodetskaya, I. A.; Grubbs, R. H. Cyclic Ruthenium-Alkylidene Catalysts for Ring-Expansion Metathesis Polymerization. *J. Am. Chem. Soc.* **2008**, *130* (38), 12775−12782.
(94) Jafari, M. G.; B. Russell, J.; Lee, H.; Pudasaini, B.; Pal, D.; Miao, Z.; R. Gau, M.; J. Carroll, P.; S. Sumerlin, B.; S. Veige, A.; Baik, M.-H.; J. Mindiola, D. Vanadium Alkylidyne Initiated Cyclic Polymer Synthesis: The Importance of a Deprotiovanadacyclobutadiene Moiety. *J. Am. Chem. Soc.* **2024**, *146* (5), 2997−3009.
(95) Rosebrugh, L. E.; Marx, V. M.; Keitz, B. K.; Grubbs, R. H. Synthesis of Highly Cis, Syndiotactic Polymers via Ring-Opening Metathesis Polymerization Using Ruthenium Metathesis Catalysts. *J. Am. Chem. Soc.* **2013**, *135* (27), 10032−10035.
(96) Rosebrugh, L. E.; Ahmed, T. S.; Marx, V. M.; Hartung, J.; Liu, P.; López, J. G.; Houk, K. N.; Grubbs, R. H. Probing Stereoselectivity in Ring-Opening Metathesis Polymerization Mediated by Cyclometalated Ruthenium-Based Catalysts: A Combined Experimental and Computational Study. *J. Am. Chem. Soc.* **2016**, *138* (4), 1394−1405.
(97) Bloomfield, V.; Zimm, B. H. Viscosity, Sedimentation, et Cetera, of Ring- and Straight-Chain Polymers in Dilute Solution. *J. Chem. Phys.* **1966**, *44* (1), 315−323.
(98) Fukatsu, M.; Kurata, M. Hydrodynamic Properties of Flexible-Ring Macromolecules. *J. Chem. Phys.* **1966**, *44* (12), 4539−4545.
(99) Rubio, A. M.; Freire, J. J.; Bishop, M.; Clarke, J. H. R. Θ State, Transition Curves, and Conformational Properties of Cyclic Chains. *Macromolecules* **1995**, *28* (7), 2240−2246.
(100) Roovers, J. Dilute-Solution Properties of Ring Polystyrenes. *J. Polym. Sci.* **1985**, *23*, 1117−1126.
(101) McKenna, G. B.; Hadziioannou, G.; Lutz, P.; Hild, G.; Strazielle, C.; Straupe, C.; Rempp, P.; Kovacs, A. J. Dilute Solution Characterization of Cyclic Polystyrene Molecules and Their Zero-Shear Viscosity in the Melt. *Macromolecules* **1987**, *20* (3), 498−512.
(102) Konar, D.; Jakhar, V. K.; Stewart, K. A.; Lester, D. W.; Veige, A. S.; Sumerlin, B. S. Functionalized Cyclic Polymers and Network Gels. *Macromolecules* **2024**, *57* (4), 1779−1787.
(103) Geiser, D.; Höcker, H. Synthesis and Investigation of Macrocyclic Polystyrene. *Macromolecules* **1980**, *13* (3), 653−656.
(104) Lutz, P.; McKenna, G. B.; Rempp, P.; Strazielle, C. Solution Properties of Ring-shaped Polystyrenes. *Makromol. Chem., Rapid Commun.* **1986**, *7* (9), 599−605.
(105) Zimm, B. H.; Stockmayer, W. H. The Dimensions of Chain Molecules Containing Branches and Rings. *J. Chem. Phys.* **1949**, *17* (12), 1301−1314.
(106) Hyvl, J.; Autenrieth, B.; Schrock, R. R. Proof of Tacticity of Stereoregular ROMP Polymers through Post Polymerization Modification. *Macromolecules* **2015**, *48* (9), 3148−3152.

https://doi.org/10.1021/acs.inorgchem.4c01522
Inorg. Chem. 2024, 63, 12207−12217